Accepted Manuscript

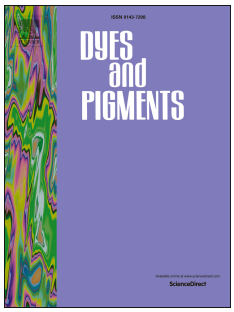

Chemiluminescence properties of luminol related quinoxaline analogues: experimental and DFT based approach to photophysical properties

Mininath S. Deshmukh, Nagaiyan Sekar

PII: S0143-7208(15)00042-X

DOI: 10.1016/j.dyepig.2015.02.006

Reference: DYPI 4660

To appear in: *Dyes and Pigments*

Received Date: 5 October 2014

Revised Date: 12 January 2015

Accepted Date: 6 February 2015

Please cite this article as: Deshmukh MS, Sekar N, Chemiluminescence properties of luminol related quinoxaline analogues: experimental and DFT based approach to photophysical properties, *Dyes and Pigments* (2015), doi: 10.1016/j.dyepig.2015.02.006.

Chemiluminescence properties of luminol related quinoxaline analogues: experimental and DFT based approach to photophysical properties

Mininath S. Deshmukh, Nagaiyan Sekar*

Tinctorial Chemistry Group, Department of Dyestuff Technology,

Institute of Chemical Technology, Nathalal Parekh Marg, Matunga, Mumbai - 400 019. (India)

*Corresponding author. Tel.: +91 22 3361 1111/2222, 2707(direct), Fax.: +91 22 3361 1020.

E-mail: n.sekar@ictmumbai.edu.in, nethi.sekar@gmail.com

Abstract:

Novel luminol and isoluminol related compounds containing a quinoxaline moiety were synthesized by the reaction of various 1,2-diketones with dimethyl-4,5-diaminophthalate **(5)** and dimethyl-3,4-diaminophthalate **(5')**. The UV-Vis absorption and emission spectra of the dyes were studied in solvents of differing polarity and the compounds show solvatofluorism properties. The chemiluminescent properties of the isoluminol and luminol based quinoxaline derivatives were examined and compared with isoluminol and luminol. These compounds produced chemiluminescence by reaction with hydrogen peroxide in the presence of potassium hexacyanoferrate(III) in sodium hydroxide solution. The chemiluminescence intensities of these chemiluminophores were affected by the concentrations of hydrogen peroxide, potassium hexacyanoferrate(III) and sodium hydroxide. These quinoxaline derivatives were found to produce chemiluminescence in the range of 3.2-7.3 and it is 0.57-1.7 times more intensely than isoluminol and luminol, respectively. Density Functional Theory computations have been used for in-depth understanding of structural, molecular, electronic and photophysical parameters of the compounds.

Keywords: Luminol-isoluminol; Chemiluminescence, Quinoxalines; Solvatochromism; Solvatofluorism; TD-DFT.

1. Introduction

5-Amino-2,3-dihydro-1,4-phthalazine-1,4-dione (luminol) and 6-amino-2,3-dihydro-1,4-phthalazine-1,4-dione (isoluminol) are the well-known chemiluminescence (CL) compounds, and their derivatives have been widely used for various biomicroanalyses due to their high selectivity and sensitivity[1]. In recent years, chemiluminescence has been an attractive detection technique for high-performance liquid chromatography (HPLC)[2]. A convenient labeling reagent having a luminol moiety has not been reported due to the fact that the CL intensity is always low and they are not so easily synthetically accessible. On the other hand, various reagents containing an isoluminol moiety like isoluminolisothiocyanate (ILITC)[3], *N*-aminobutyl-*N*-ethylisoluminol (ABEI)[4,5], 4,5-diaminophthalhydrazide (DPH)[6] and 6-aminomethylphthalhydrazide (6-AMP)[7] have been widely used for the microanalyses of biological compounds. The most of these reagents react with the amino and carboxylic acid groups of the analytes and a new CL labeling reagent which reacts with the other functional groups is required. The modification of the amino group of luminol with the electron donating groups such as an alkyl or aryl group causes a decrease in the CL intensity. On the other hand, that of the isoluminol with an electron donating group causes an increase in the CL intensity[8,9].

The quinoxaline derivatives are also an important class of benzoheterocycles have been widely used as dyes[10], emitters in organic light emitting diodes, building blocks of organic semiconducting constituents in thin-film transistors[11], as well as fluorescent sensors and π-conjugating chromophores in nonlinear optical materials[12–14]. There exists an extensive π-conjugation in quinoxaline based chromophores and they display a strong emission with relatively low Stokes shifts. But, in the planar structure, they are prone to stronger intermolecular π-π stacking interactions, which often decrease their luminescence and increase the tendency to form crystals in the solid state[15] While the stacking interactions are beneficial for the charge transport properties, crystallinity and decrease in emission yield

or unwanted red-shift in emission in the solid state pose a problem in the utilization of polyaromatic hydrocarbon in organic light-emitting diodes[16–18].

In this paper we report the synthesis of π-conjugated luminol and isoluminol based quinoxaline chromophores with relatively high Stokes shifts. The molecular structures are shown in **Scheme 1.** These dyes were obtained by the condensation reaction between dimethyl 4,5-diaminophthalate or dimethyl 3,4-diaminophthalate and different substituted 1,2-diketone **(a-c).** Density functional theory computations [B3LYP/6-31G(d)] were used to study the geometrical and electronic properties of the synthesized molecules. Their structures were confirmed by FT-IR, ^{1}H NMR and mass spectra. Their thermal stability, UV-Vis absorption, emission and chemiluminescence characteristics were also studied.

2. Experimental Section

2.1. Materials and Methods

All the commercial reagents and the solvents were purchased from S. D. Fine Chemicals Pvt. Ltd. and were used without purification. The reaction was monitored by TLC using on 0.25 mm silica gel 60 F_{254} precoated plates, which were visualized with UV light. Melting points were measured on standard melting point apparatus from Sunder industrial product Mumbai and are uncorrected. FT-IR spectra were recorded on Jasco 4100 using ATR accessory. ^{1}H-NMR spectra were recorded on VARIAN Inc. (USA) 400/500/600-MHz instrument using TMS as an internal standard and $CDCl_3$/DMSO-d_6 as the solvent at room temperature. Mass spectra were recorded on Finnigan mass spectrometer. Simultaneous DSC-TGA measurements were performed out on SDT Q 600 v8.2 Build 100 model of TA instruments Waters (India) Pvt. Ltd. The UV-visible absorption and emission, chemiluminescence spectra were performed on a Perkins-Elmer Lamda 25 and Varian Cary Eclipse at room temperature respectively. Quantum yields were obtained by using quinine sulfate (0.54 in 0.1 M H_2SO_4) as reference[19].

Stock solutions ($1x10^{-3}$ M) of each chemiluminophore were prepared in *N*,*N*-dimethylformamide (DMF) and these solutions were stable for at least 2 weeks. The solutions of potassium hexacyanoferrate(III) (2.0-50 mM) and hydrogen peroxide (2.0-50 mM) were prepared in sodium hydroxide (0.5-3.0M) solution and used within 12 h.

2.2. Computational methods

The ground state (So) geometry of the synthesized compounds were optimized in vacuum using Density Functional Theory (DFT)[20]. The functional used was B3LYP. The B3LYP method combines Becke's three parameter exchange functional (B3)[21] with the nonlocal correlation functional by Lee, Yang, and Parr (LYP)[22]. The basis set used for all the atoms was 6-31G(d), the latter has been justified in the literature[23–25] for the current investigation. The vibrational frequencies at the optimized structures were computed using the same method to verify that the optimized structures correspond to local minima on the energy surface[26]. The vertical excitation energy and oscillator strengths at ground state equilibrium geometries were calculated by using TD-DFT at the same hybrid functional and basis set[27–29]. The low-lying first singlet excited states (S1) of dyes was relaxed using TD-DFT to obtain its minimum energy geometry. The difference between the energies of the optimized geometries at the first singlet excited state and the ground state was used in computing the emissions[30,31]. Frequency computations were also carried out on the optimized geometry of the low-lying vibronically relaxed first excited state of conformers. All the computations in solvents of different polarities were carried out using the Polarizable Continuum Model (PCM)[32]. All electronic structure computations were carried out using the Gaussian 09 program[33].

2.3. Synthetic strategy

The compounds **7a-7c, 7'a-7'c, 8a-8c** and **8'a-8'c** contain the donor core 9,10-dihydrophenanthrene/ 1,2-diphenylethane/ 1-ethylindoline along with quinoxaline unit and the diester acceptor moiety. They were synthesized by the conventional condensation of dimethyl 4,5-diaminophthalate (**6**) and dimethyl 4,3-diaminophthalate (**6'**) with the different 1,2-diketones **(a-c) (Scheme 1).**

In the first step, dimethyl-4-nitrophthalate **1** was synthesized by the esterification of 4-nitrophthalic acid. The compound **1** on reduction by using H_2- Pd/C (10%) gave the compound **2,** which on further acetylation using acetic anhydride in toluene yielded the intermediate **3**. Nitration of the intermediate **3** with fuming HNO_3 and H_2SO_4 gave the intermediates **4** and **4'**, which on deacetylation in concentrated H_2SO_4 gave the intermediates **5** and **5'.** Nitro group of the compounds **5** and **5'** was reduced using H_2- Pd/C (10%) to give the compounds **6** and **6',** which on further condensation with the 1,2-diketones **(a-c)** in glacial acetic acid at reflux temperature gave the compounds **7a-7b** and **7'a-7'c.** Finally the compound was refluxed in hydrazine hydrate and triethyl amine in methanol to yield the desired chemiluminescent compounds **8a-8b** and **8'a-8'c** respectively**.**

<< Please insert Scheme 1 >>

2.4. Examination of the chemiluminescent properties

2.4.1. Standard procedure

The chemiluminescence reaction was initiated by the simultaneous automatic injections of 100 µl of hydrogen peroxide solution and 100 ml of potassium hexacyanoferrate(III) solution dissolved in sodium hydroxide to the 100 µl portion of a 10 nM solution of each chemiluminophore **(Figure 1)**. The chemiluminescence intensities were recorded immediately after the injection of oxidizing agent solution.

The integrated photon counts for 1 min after the injections were explained as the chemiluminescence intensities.

<< Please insert Figure 1 >>

2.4.2. Optimization of the chemiluminescence conditions

To establish the optimum chemiluminescence conditions the concentrations of the oxidizing reagents (hydrogen peroxide, potassium hexacyanoferrate(III) and sodium hydroxide) were varied one at a time. The temporarily settled conditions were DMF solution of chemiluminophore, 10.0 mM hydrogen peroxide and 10.0 mM potassium hexacyanoferrate(III) prepared in 1.5 M sodium hydroxide.

2.4.3. Fluorescence of the CL Reaction Product

To 200 µl of the 1mM stock solution of chemiluminophores, 50 µl of 10 mM potassium hexacyanoferrate(III) in 1.5 M NaOH and 50 µl of 10mM hydrogen peroxide were added and allowed to stand for 1 h at room temperature. The emission maxima, excitation and relative intensities of the resulting mixtures were recorded in the fluorescence spectrometer.

2.5. Synthesis and characterization

The synthetic scheme for the preparation of luminol-isoluminol based quinoxaline derivatives are shown in **Scheme 1**. Dimethyl 4,5-diaminophthalate (**6**) and dimethyl 4,3-diaminophthalate (**6'**) were prepared by the reported procedure[34] from 4-nitrophthalic acid.

2.5.1. General procedure for the preparation of quinoxalines

Diamino-dimethylphthalate **(6** or **6')** 0.5 g (2.2 mmol) and substituted 1,2-diketones (**a-c)** (2.2 mmol) were dissolved in acetic acid (5 mL), and the reaction mixture was refluxed for 6 h. The mixture was poured on the crushed ice and the precipitate obtained was filtered, washed with water and dried to afford **7a-7c** and **7'a-7'c**. The product was recrystalized from ethanol.

Dimethyl dibenzo[a,c]phenazine-11,12-dicarboxylate **(7a):**

Yield: 92%; Melting point: 260-262 ^{o}C; HRMS: Calcd for $C_{24}H_{16}N_2O_4Na$ $[M+Na]^+$ 419.1008, found 419.1008; FAB-MS m/z: 397.47 $[M+H]^+$; ^{1}H NMR ($CDCl_3$, 600 MHz): δ 9.39 (d, 2H, Ar-H, *J* = 7.8 Hz), 8.72 (s, 2H, Ar-H), 8.58 (d, 2H, Ar-H, *J* = 8.4 Hz), 7.86 (t, 2H, Ar-H, *J* = 7.8 Hz), 7.78 (t, 2H, Ar-H, *J* = 7.8 Hz), 4.04 (s, 6H, -OCH_3); ^{13}C NMR ($CDCl_3$, 125.8 MHz): δ 167.78, 145.12, 133.63, 131.22, 130.03, 128.75, 127.15, 126.34, 125.87, 124.72, 121.41, 52.07; FT-IR: 1737, 1722 (-C=O ester), 1609, 1569 (C=C, C=N ring stretching), 1271, 1258 (C-O stretching) cm^{-1}.

Dimethyl 2,3-diphenylquinoxaline-6,7-dicarboxylate **(7b):**

Yield: 87%; Melting point: 214-216 ^{o}C; HRMS: Calcd for $C_{24}H_{19}N_2O_4$ $[M+H]^+$ 399.1345, found 399.1343; FAB-MS m/z: 399.33 $[M+H]^+$; ^{1}H NMR ($CDCl_3$, 600 MHz): δ 8.56 (s, 2H, Ar-H), 7.55 (m, 4H, Ar-H), 7.39 (m, 6H, Ar-H), 4.00 (s, 6H, -OCH_3); ^{13}C NMR ($CDCl_3$, 125.8 MHz): δ 167.92, 157.63, 144.06, 137.53, 132.43, 131.92, 130.23, 129.41, 128.95, 128.35, 127.21, 51.67; FT-IR: 1740, 1725 (-C=O ester), 1615, 1589 (C=C, C=N ring stretching), 1261, 1240 (C-O stretching) cm^{-1}.

***Dimethyl 6-ethyl-6H-indolo[2,3-b]quinoxaline-2,3-dicarboxylate* (7c):**

Yield: 90%; Melting point: 184-186 ^{o}C; HRMS: Calcd for $C_{20}H_{17}N_3O_4Na$ $[M+Na]^+$ 386.1117, found 386.1116; FAB-MS m/z: 364.47 $[M+H]^+$; ^{1}H NMR ($CDCl_3$, 600 MHz): δ 8.75 (s, 1H, Ar-H), 8.51 (d, 1H, Ar-H, *J* = 7.8 Hz), 8.46 (s, 1H, Ar-H), 7.78 (t, 1H, Ar-H, *J*= 9.0 Hz), 7.54 (d, 1H, Ar-H, *J* = 7.2 Hz), 7.78 (t, 1H, Ar-H, *J*= 7.8 Hz), 4.59 (q, 2H, -NCH_2), 4.01 (s, 6H, -OCH_3), 1.55 (t, 3H, -CH_3); ^{13}C NMR ($CDCl_3$, 125.8 MHz): δ 167.83(s), 147.51, 145.12, 142.73(s), 110.13, 132.51(s), 129.83(s), 124.07, 123.45, 121.65, 120.93, 110.17, 52.73, 52.08, 47.35, 14.32; FT-IR: 1745, 1739 (-C=O ester), 1621, 1595 (C=C, C=N ring stretching), 1267, 1242 (C-O stretching) cm^{-1}.

***Dimethyl dibenzo[a,c]phenazine-10,11-dicarboxylate* (7'a):**

Yield: 85%; Melting point: 254-256 ^{o}C; HRMS: Calcd for $C_{24}H_{16}N_2O_4Na$ $[M+Na]^+$ 419.1008, found 419.1013; Mass m/z: 397.40 $[M+H]^+$; ^{1}H NMR ($CDCl_3$, 400 MHz): δ 9.39 (d, 1H, Ar-H, *J* = 8.0 Hz), 9.29 (d, 1H, Ar-H, *J* = 8.0 Hz), 8.55 (t, 2H, Ar-H, *J*= 7.2 Hz), 8.41 (s, 2H, Ar-H), 7.84 (dd, 2H, Ar-H, *J* = 7.2 Hz and *J* = 8.0 Hz), 7.75 (t, 2H, Ar-H, *J* = 7.2 Hz and *J* = 8.0 Hz), 4.25 (s, 3H, -OCH_3), 4.05 (s, 3H, -OCH_3); ^{13}C NMR ($CDCl_3$, 125.8 MHz): δ 167.34, 162,95, 144.05, 139.12(s), 138.27(s), 136.84, 135.66, 132.72, 131.45 (s), 130.14(s), 129.17(s), 128.55, 128.17(s), 127.69(s), 126.04, 52.07, 51.63; FT-IR: 1735, 1722 (-C=O ester), 1614, 1578 (C=C, C=N ring stretching), 1280, 1244 (C-O stretching) cm^{-1}.

***Dimethyl 2,3-diphenylquinoxaline-5,6-dicarboxylate* (7'b):**

Yield: 80%; Melting point: 202-204 ^{o}C; HRMS: Calcd for $C_{24}H_{18}N_2O_4Na$ $[M+Na]^+$ 421.1164, found 421.1159; FAB-MS m/z: 399.20 $[M+H]^+$; ^{1}H NMR ($CDCl_3$, 400 MHz): δ 8.33 (d, 1H, Ar-H, *J* = 9.2 Hz), 8.23 (d, 1H, Ar-H, *J* = 9.2 Hz), 7.55 (d, 4H, Ar-H, *J* = 6.8 Hz), 7.35 (m, 6H, Ar-H), 4.09 (s, 3H, -OCH_3), 4.01 (s, 3H, -OCH_3); ^{13}C NMR ($CDCl_3$, 125.8 MHz): δ 167.22, 163,75, 157.13, 148.13, 144.05,

139.51(s), 137.83, 135.17, 134.02, 133.63, 131.13(s), 131.77(s), 129.44, 128.36(s), 127.61(s), 125.10, 52.33, 51.94; FT-IR: 1741, 1730 (-C=O ester), 1621, 1577 (C=C, C=N ring stretching), 1251, 1232 (C-O stretching) cm^{-1}.

Dimethyl 6-ethyl-6H-indolo[2,3-b]quinoxaline-3,4-dicarboxylate **(7'c):**

Yield: 85%; Melting point: 176-178 ^{o}C; HRMS: Calcd for $C_{20}H_{17}N_3O_4Na$ $[M+Na]^+$ 386.1117, found 386.1114; FAB-MS m/z: 364.42 $[M+H]^+$; ^{1}H NMR ($CDCl_3$, 400 MHz): 8.46 (d, 1H, Ar-H, *J* = 8.0 Hz), 8.34 (d, 1H, Ar-H, *J* = 8.8 Hz), 8.18 (d, 1H, Ar-H, *J* = 8.8 Hz), 7.74 (t, 1H, Ar-H, *J* = 8.4 Hz), 7.50 (d, 1H, Ar-H, *J* = 8.0 Hz), 7.78 (t, 1H, Ar-H, *J* = 8.4 Hz), 4.58 (q, 2H, -NCH_2), 4.19 (s, 3H, -OCH_3), 4.01 (s, 3H, -OCH_3), 1.55 (t, 3H, -CH_3); ^{13}C NMR ($CDCl_3$, 125.8 MHz): δ 167.62, 162,95, 148.03, 145.13, 144.36, 137.23, 136.93, 135.67, 134.81, 132.13, 126.61, 123.77, 123.18, 119.74, 119,08, 110.11, 52.67, 52.03, 47.16, 14.28; FT-IR: 1748, 1732 (-C=O ester), 1614, 1571 (C=C, C=N ring stretching), 1254, 1232 (C-O stretching) cm^{-1}.

2.6.2. General procedure for the preparation of phthalazines (8a-8c and **8'a-8'c):**

The compounds **7a-7c** and **7'a-7'c** (1 mmol) and hydrazine hydrates (1.5 ml) were reacted in the presence of triethyl amine (1.5 ml) in methanol (5 ml) at reflux temperature for 2 h. The product was precipitated during reflux temperature or at room temperature. The crude product was recrystallized from *N,N*'-dimethylacetamide to get the compounds **8a-8c** and **8'a-8'c.** The low solubility of the compounds **8a-8c** and **8'a-8'c** made the ^{13}C-NMR characterization of these substrates not possible. Only the ^{1}H-NMR, HRMS and IR are recorded.

12,13-Dihydrodibenzo[a,c]pyridazino[4,5-i]phenazine-11,14-dione **(8a):**

Yield: 86%; Melting point: > 300 ^{o}C; HRMS: Calcd for $C_{22}H_{13}N_4O_2$ $[M+H]^+$ 365.1039, found 365.1041; FAB-MS m/z: 364.40 $[M]^+$; ^{1}H NMR (DMSO-d_6, 600 MHz): 11.00 (brs, 2H, -NH), 9.32 (d, 2H, Ar-H, *J* = 7.8 Hz), 8.91 (s, 2H, Ar-H), 8.81(d, 2H, Ar-H, *J* = 8.4 Hz), 7.92 (t, 2H, Ar-H, *J* = 7.8 Hz), 7.85 (d, 2H, Ar-H, *J* = 7.2 Hz); FT-IR: 3014, 2897 (N-H amide), 1665, 1625 (-C=O amide), 1602, 1536 (C=C, C=N ring stretching), 1315, 1268 (C-N stretching) cm^{-1}.

2,3-Diphenyl-7,8-dihydropyridazino[4,5-g]quinoxaline-6,9-dione **(8b):**

Yield: 84%; Melting point: > 300 ^{o}C; HRMS: Calcd for $C_{22}H_{15}N_4O_2$ $[M+H]^+$ 367.1195, found 367.1149; FAB-MS m/z: 367.27 $[M+H]^+$; ^{1}H NMR (DMSO-d_6, 600 MHz): 11.76 (s, 2H, -NH), 8.83 (s, 1H, Ar-H), 8.64 (s, 1H, Ar-H), 7.53 (d, 4H, Ar-H, *J* = 7.8 Hz), 7.43 (t, 2H, Ar-H, *J* = 7.2 Hz), 7.38 (t, 4H, Ar-H, *J* = 7.2 Hz); FT-IR: 3014, 2893 (N-H amide), 1661, 1626 (-C=O amide), 1600, 1595 (C=C, C=N ring stretching), 1366, 1340 (C-N stretching) cm^{-1}.

7-Ethyl-2,3-dihydro-1H-indolo[2,3-b]pyridazino[4,5-g]quinoxaline-1,4(7H)-dione **(8c):**

Yield: 77%; Melting point: > 300 ^{o}C; HRMS: Calcd for $C_{18}H_{15}N_5O_2$ $[M+2H]^+$ 333.1226, found 333.2879; FAB-MS m/z: 332.23 $[M+H]^+$; ^{1}H NMR (DMSO-d_6, 600 MHz): 11.56 (brs, 2H, -NH), 8.88 (s, 1H, Ar-H), 8.68 (s, 1H, Ar-H), 8.42 (d, 1H, Ar-H, *J* = 7.8 Hz), 7.83 (s, 2H, Ar-H), 7.44 (t, 1H, Ar-H, *J* = 5.4 Hz), 4.54 (q, 2H, -NCH_2), 1.43 (t, 3H, -CH_3); FT-IR: 3029, 2903 (N-H amide), 1660 (-C=O amide), 1613, 1578 (C=C, C=N ring stretching), 1315, 1241 (C-N stretching) cm^{-1}.

2,3-Dihydrodibenzo[a,c]pyridazino[4,5-h]phenazine-1,4-dione **(8'a):**

Yield: 80%; Melting point: > 300 ^{o}C; HRMS: Calcd for $C_{24}H_{15}N_5O_2$ $[M+CH_3CN]^+$ 405.1226, found 405.1351; FAB-MS m/z: 364.40 $[M+H]^+$; ^{1}H NMR (DMSO-d_6, 600 MHz): 13.31 (s, 1H, -NH), 12.54 (s, 1H, -NH), 9.58 (d, 2H, Ar-H, J = 7.8 Hz), 8.56 (d, 1H, Ar-H, J = 7.2 Hz), 8.24 (d, 1H, Ar-H, J = 7.2 Hz), 7.91(d, 2H, Ar-H, J = 7.8 Hz), 7.64 (t, 2H, Ar-H, J = 7.2 Hz), 7.35 (d, 2H, Ar-H, J = 7.8 Hz); FT-IR: 3160, 3009 (N-H amide), 1670, 1649 (-C=O amide), 1602, 1567 (C=C, C=N ring stretching), 1356, 1283 (C-N stretching) cm^{-1}.

7-Hydroxy-2,3-diphenyl-8,9-dihydropyridazino[4,5-f]quinoxalin-10(7H)-one **(8'b):**

Yield: 78%; Melting point: > 300 ^{o}C; HRMS: Calcd for $C_{22}H_{15}N_4O_2$ $[M+H]^+$ 367.1195, found 367.1196; FAB-MS m/z: 389.27 $[M+Na]^+$; ^{1}H NMR (DMSO-d_6, 600 MHz): 12.88 (s, 1H, -NH), 12.42 (s, 1H, -NH), 8.56 (dd, 2H, Ar-H, J = 9.0 Hz and J = 9.6 Hz), 7.55 (t, 4H, Ar-H, J = 6.0 Hz), 7.50 (t, 2H, Ar-H, J = 7.2 Hz), 7.46 (t, 2H, Ar-H, J = 6.6 Hz), 7.41 (t, 2H, Ar-H, J = 7.8 Hz); FT-IR: 3055, 2903 (N-H amide), 1665 (-C=O amide), 1602, 1564 (C=C, C=N ring stretching), 1354, 1294 (C-N stretching) cm^{-1}.

12-Ethyl-2,3-dihydro-1H-indolo[3,2-b]pyridazino[4,5-f]quinoxaline-1,4(12H)-dione **(8'c):**

Yield: 82%; Melting point: > 300 ^{o}C; HRMS: Calcd for $C_{18}H_{14}N_5O_2$ $[M+H]^+$ 332.1147, found 332.1145; FAB-MS m/z: 332.20 $[M+H]^+$; ^{1}H NMR (DMSO-d_6, 600 MHz): 13.29 (s, 1H, -NH), 12.28 (s, 1H, -NH), 8.58 (d, 1H, Ar-H, J = 7.8 Hz), 8.50 (s, 2H, Ar-H), 7.95 (d, 1H, Ar-H, J = 7.8 Hz), 7.90 (t, 1H, Ar-H, J = 7.8 Hz), 7.52 (t, 1H, Ar-H, J = 7.8 Hz), 4.63 (q, 2H, -NCH_2), 1.45 (t, 3H, -CH_3); FT-IR: 3042, 2897 (N-H amide), 1654, 1617 (-C=O amide), 1580, 1560 (C=C, C=N ring stretching), 1330, 1295 (C-N stretching) cm^{-1}.

3. Results and discussion:

3.1. Photo-physical properties

The UV-Vis absorption and emission spectra of the phthalate and luminol-isoluminol related quinoxaline compounds in the solvents of varying polarities are reported in **Tables S1-S7**. The phthalate quinoxaline derivatives have the solubility mostly in all the organic solvents but luminol-isoluminol quinoxaline have the solubility only in highly polar solvents like DMF and DMSO. The absorption spectra of the compounds in all the studied solvents are almost nearly the same; their absorption property is independent of the solvent polarity **(Figure S1-S12).** The rigidity in the structure exhibited a strong red-shifted absorption shown in **Figure 2, Tables 1, S1-S7.** The compounds **7a, 7c, 7'a, 7'c** and **8a, 8c, 8'a, 8'c** have four absorption maxima. Among these four transitions, first three are higher energy absorptions between 270 nm-380 nm probably due to the π-π* and n- π* transition while the lower energy band between 390 nm and 410 nm attributed to the intramolecular charge transfer transition (ICT) between the donor group and the acceptor moiety. Also, all these compounds exhibit highly intense first absorption peak at 270-300 nm due to the aryl core[35], while the absorption spectra of the compounds **7b 7'b** and **8b, 8'b** contain two absorption maxima. Among these two, the first one is a high energy absorptions between 270 nm-320 nm probably due to the π-π* transition while the low energy band between 320 nm and 370 nm is attributed to the intramolecular charge transfer transition (ICT).

The emission spectra of the compounds **7a, 7c, 7'a, 7'c** and **8a, 8c, 8'a, 8'c** exhibited a strong solvent effect as compared to the compounds **7b, 7'b** and **8b, 8'b**. In the protonated solvents all the compounds show emission maxima at longer wavelengths than in the other solvents (**Tables S1-S7, Figures S1-S12)**. In the polar solvents like methanol, DMF the emissive S1 state with intramolecular charge transfer (ICT) character is strongly solvated and its energy is dramatically lowered. The rigidity in the molecules **7a, 7c, 7'a, 7'c** and **8a, 8c, 8'a, 8'c** leads to a red shift (lower energy) in the emission

(Figure 3). The extent of red shift in emission of the above molecules is more as compared to the red shift in the corresponding absorption values which may be attributed to more energy losses due to dissipation of the vibrational energy during the decay and is influenced by the interaction between the fluorophore and the solvent molecules around the excited dipole, hydrogen bonding and the formation of charge complexes.

<< Please insert Figure 2 >>

<< Please insert Figure 3>>

<< Please insert Table 1>>

3.2. Quantum yield of Compounds:

The fluorescence quantum yields of the synthesized quinoxaline compounds were determined in different solvents and tabulated in **Tables 1, S1-S7**. The fluorescence quantum yields of the compounds are mostly depending on both the nature of the substituent and the solvent polarity. Here, it has been observed that the compounds **7a-7c, 7'a-7'b** and compounds **8a-8c, 8'a-8'c** enhances the fluorescence quantum yields in the polar protic (ethanol) and polar aprotic (DMF) solvent respectively. The dyes showed higher quantum efficiencies in the non-polar solvents while lower quantum yields in the polar solvents. The highest quantum yield of the compounds **7a-7c, 7'a-7'c** and **8a-8c, 8'a-8'c** was observed in ethanol and DMF and the values in the increasing order are: **7'b** (0.04) < **7'a** (0.07) = **7'a** (0.07) < **7a** (0.12) < **7'c** (0.13) < **7c** (0.15) and 7'b (0.04) < **7c** (0.08) = **7'c** (0.08) < **7a** (0.09) < **8a**(0.10) = **8'a**(0.10). The quantum yield values were the lowest in DCM in the decreasing order: **7'c** (0.11) > **8'a** (0.10) > **7a** (0.09) = **7c** (0.09) > **8c** (0.07) > **8a** (0.06) = **8'c** (0.06) > **7'a** (0.05) = **8b** (0.05) > **7b** (0.04) > **7'b** (0.03) = 8'b (0.03). These compounds showed comparatively less emission intensity in acetonitrile, DMSO and DMF showing a clear positive solvatokinetic behavior suggesting that a highly polar excited-state population charge transfer state and a non-radiative decay was prominent in these compounds[30].

3.3. Chemiluminescence Study

The chemiluminescence properties of isoluminol-luminol type of derivatives **8a-8c** and **8'a-8'c** were examined in order to evaluate their use as highly chemiluminescent probes. These six compounds, like luminol and isoluminol produce chemiluminescence by the reaction with hydrogen peroxide in the presence of potassium hexacyanoferrate(III) in alkaline medium**.** The concentrations of the three oxidizing reagent systems have a major influence on the chemiluminescence intensity **(Figure 4);** 2.5-20 mM hydrogen peroxide, 2.5-20 mM potassium hexacyanoferrate(III) and 0.5-2.0 M sodium hydroxide give the maximum intensity. After the addition of hydrogen peroxide and potassium hexacyanoferrate(III) the chemiluminescence intensity reaches a maximum in a few seconds and then almost disappears within one minute.

Under these optimum reaction conditions, the chemiluminescence intensities of the six compounds are determined **(Table 2).** The generation of the chemiluminescence of the compounds **8a-8c** and **8'a-8'c** are found approximately 3.2-7.3 times larger than that of the isoluminol, and the intensities corresponded to 0.57-1.7 times of that obtained with the luminol. The time dependence of the chemiluminescence reaction of the synthesized compounds and luminol-isoluminol is illustrated in **Figure 5.** The generation of chemiluminescence is initiated by the addition of hydrogen peroxide and potassium hexacyanoferrate(III) in alkaline solutions to the stock solution. The chemiluminescence intensity was maximum at <1.5 s after the addition of the oxidizing reagents, and then decreased rapidly. In the chemiluminescence of luminol and isoluminol, the 3-aminophthalate and 4-aminophthalate ion produced during the oxidizing reaction have been shown to be the light emitter. Therefore, the newly synthesized luminol-isoluminol type compounds, and the corresponding dicarboxylate ions **(Figure 1)** could be expected to be the light emitting species. The excitation and emission maxima of the

fluorescence and the relative intensity of the chemiluminescent species on the completion of the chemiluminescence reaction are measured, and compared with the conventional luminol analogues **(Table 2)**. The fluorescence intensities of the dicarboxylate ions of the quinoxaline derivatives are 1.1-12.5 times larger than that of 3-aminophthalate anion of the luminol. The result proposes that the efficiency of the chemiluminescencent compound is mostly dependent on the fluorescence intensities of the light-emitting species produced during the reaction. Otherwise, it is known that the chemiluminescence spectra of the isoluminol and luminol type compounds are almost identical to the emission spectra of the corresponding phthalate ion[36] **(Figure 1)**. Thus, the compounds **8a, 8c** and **8'a-8'c** are expected to generate chemiluminescence at longer wavelengths as compared to the isoluminol and luminol respectively.

<< Please insert Figure 4 >>

<< Please insert Figure 5 >>

<< Please insert Table 2 >>

3.4. Geometry optimization

The ground state geometries of the compounds **7a, 7c, 7'a, 7'c, 8a, 8c, 8'a** and **8'c** were having planar arrangement of the condense ortho-diamino with diketone due to their rigidity. While, the compounds **7b, 7'b, 8b** and **8'b** both the phenyl ring on quinoxaline is twisted. In the phthalate compounds **7a-7c** and **7'a-7'c** the ester group have small twist with the quinoxaline.

As a representative example, the structural view of the compound **7b** in the ground and the excited state in DMF is presented in **Table 3, Figure 6** and the structures of the remaining compounds are summarized in **Tables S8-S10, Figures S13-S23**. In the dye **7b** major bond lengthening was observed between the bonds C_1-C_2, C_3-N_4, C_5-C_6, C_9-O_{10}, C_{20}-C_{25}, C_{22}-C_{21}, C_{29}-N_{19} by 0.032, 0.018, 0.003, 0.007,

0.012, 0.012, 0.05 Å and the bond length shortened for the bonds C_2-C_6, C_4-C_5, O_{11}-C_{14}, C_{22}-C_{26}, C_{23}-C_{24}, C_{26}-C_{29} by 0.012, 0.003, 0.002, 0.02, 0.007, 0.039 Å. Such a lengthening and shortening of the bonds are due to the effective charge delocalization in the molecules. Also, the excited state twist dihedral angle of both the phenyl ring with quinoxaline unit was reduced to maintain the planarity.

<< Please insert Figure 6 >>

<< Please insert Table 3 >>

Twisted geometry in the compounds 7b, 7'b, 8b and 8'b

The ground state optimized geometry of the dyes **7b, 7'b, 8b** and **8'b** in DMF has a dihedral angle between both the phenyl ring and the quinoxaline C_{23}-C_{22}-C_{26}-C_{29}/C_{27}-C_{28}-C_{29}-C_{26} 40^o-44^o. The ester groups of the compounds **7a-7c** and **7'a-7'c** have a larger dihedral angle with the quinoxaline unit than the fused phthalazine based quinoxaline compounds **8a-8c** and **8'a-8'c**. In the excited state of the compounds **7b, 7'b, 8b** and **8'b** in DMF both the phenyl ring was twisted to a reduced dihedral angle between C_{23}-C_{22}-C_{26}-C_{29}/C_{27}-C_{28}-C_{29}-C_{26} up to 31^o-38^o. Similarly the terminal ester and 1,2-dihydropyridazine-3,6-dione are also twisted to a reduced dihedral angle amounting to reaching a planarity in the excited state **(Table 4)**.

<< Please insert Table 4 >>

The Mulliken charge distribution in the ground and excited state (DMF solvent) of all the compounds are summarized in **Tables S11-S14, Figures S24-S34.** In the excited state of the compound **7a,** net positive charge on the atom C_{26} and C_{29} increases from 0.257 to 0.263. Also the net negative charge on $N_{18/19}$ and C_3 atom increases from -0.606 to -0.608 and -0.220 to -0.224 (in au) **(Figure 7)**,The above observations are suggestive of charge delocalization in the compounds **7a-7c**, **7'a-7'c** and **8a-8c, 8'a-**

8'c from different donor 9,10-dihydrophenanthrene/ 1,2-diphenylethane/ 1-ethylindoline along with the quinoxaline unit to the diester and the 2,3-dihydrophthalazine-1,4-dione acceptor moiety respectively. These atoms are also engaged in bond lengthening and shortening at the excited state. The structures indicating charge distribution on the dyes were visualized using GaussView 5.0 software[37].

<< Please insert Figure 7 >>

3.5. Electronic vertical excitations (TD-DFT)

The electronic vertical excitations were calculated using TD-B3LYP/6-31G(d) method. The experimental absorption wavelengths and the computed vertical excitation spectra associated with their oscillator strengths, composition, and their corresponding assignments of the compounds **7a-7c, 7'a-7'c, 8a-8c** and **8'a-8'c** are summarized in **Tables 1, S1-S7.** The absorption band occurring at a lower energy is due to the intramolecular charge transfer (ICT) and it is the characteristic of the donor-π-acceptor push-pull dyes. These ICT bands for the compounds **7a-7c, 7'a-7'c** and **8a-8c**, **8'a-8'c** were mainly due to the electronic transitions from the highest occupied molecular orbital (HOMO) and HOMO-1 to the lowest unoccupied molecular orbital (LUMO) respectively. While remaining transition assign from π-π* and n- π* is summarized in **Table S1-S7.** The experimental absorption and computed vertical excitation of the all compounds are independent on the solvent polarity, while Stokes shift increases progressively with the increase in solvent polarity. These observations are in accordance with the higher stabilization in increasingly polar protic solvents. Emission values of the compound **7a** were computed in all solvents and compounds **7b-7c, 7'a-7'c, 8a-8c** and **8'a-8'c** in DMF. The computational emission results obtained by using TD-B3LYP/6-31G(d) were not able to reproduce the solvatofluorism behavior and shown almost nearly same value of the emission energy.

As a representative example dimethylphthalate quinoxaline **7a,** experimental absorption and it's computed vertical excitation values in DMF are 410, 361, 349, 261 nm and 417, 347, 344, 300 nm due to the HOMO→LUMO, HOMO-1→LUMO, HOMO-2→LUMO, HOMO→LUMO+1 respectively. There is a significant difference (~ 14 nm) and % deviation between experimental absorption and vertical excitation is between 1.294-3.96% in studied solvents. The largest wavelength difference between experimental absorption maxima obtained from ICT and computed vertical excitation was 9 nm (DMF), 13 nm (DCM), 8 nm (acetone), 16 nm (methanol), 19 nm (DMF) and 24 nm (acetone) for compounds **7a, 7b, 7c, 7'a, 7'b** and **7'c** respectively.

The first excited state of the compounds **7a** in all the solvents and **7b-7c, 7'a-7'c, 8a-8c, 8'a-8'c** in DMF were optimized to calculate the fluorescence. The experimentally obtained emission spectral data and the emission computed from TD-B3LYP/6-31G(d) computations are shown in **Table 5**. The computational results obtained by using TD-B3LYP/6-31G(d) were not able to reproduce the solvatofluorism behavior of the dye **7a** and showed almost nearly same value of emission energy. The difference between the energies of the optimized geometries at the first singlet excited state and the ground state are used to calculate emissions are summarized in **Table S15-S16.** The experimental emission wavelength and emission computed by TD-B3LYP/6-31G(d) showed a largest difference of 58 nm in methanol and showed a closest difference of 13 nm in acetone. Similarly, difference between the experimental emission wavelength and the emission computed by TD-B3LYP/6-31G(d) in DMF of the compounds **7b, 7c, 7'a-7'c, 8a-8c** and **8'a-8'c** summarized in **(Table 6)**.

<< Please insert Table 5 >>

<< Please insert Table 6 >>

As a representative example phthalazine based quinoxaline **8a,** experimental absorption and it's computed vertical excitation values in DMF are 411, 394, 303, 267 nm and 408, 389, 316, 273 nm due to the HOMO-1→LUMO, HOMO-2→LUMO, HOMO→LUMO+1, HOMO-2→LUMO+1 respectively. There is a significant difference (~ 3 nm) and % deviation between experimental absorption and vertical excitation in DMF is 0.8 %. The wavelength difference between experimental absorption maxima obtained from ICT and the computed vertical excitation of the compounds **8b, 8c, 8'a, 8'b** and **8'c** in DMF was 14, 32, 4, 9 and 2 nm respectively **(Tables S1-S7).**

The compounds **8a-8c** and **8'a-8'c** were optimized in the first excited state to calculate the fluorescence in DMF solvent. The experimentally obtained emission spectral data and the emission computed from TD-B3LYP/6-31G(d) computations are shown in **Table 6**. The % deviation between the experimental emission wavelength and the emission computed by TD-B3LYP/6-31G(d) of the compounds **8a, 8b, 8c, 8'a, 8'b** and **8'c** in DMF is 4.4, 10.2, 7.4, 3.5, 6.5, 4.5, 3.6, 3.6, 11.4, 1.6 and 8.0 respectively.

3.6. Frontier molecular orbitals

The different frontier molecular orbitals were studied to understand the electronic transition and charge delocalization within the molecules. The comparative increase and decrease in the energy of the occupied (HOMO's) and virtual orbitals (LUMO's) gives a qualitative idea of the excitation properties and the ability of the hole or electron injection[10]. The first allowed and the strongest electron transitions usually correspond almost exclusively to the ICT of an electron from HOMO → LUMO and HOMO-1 → LUMO for dimethylphthalate and phthalazine quinoxaline respectively (**Table S1-S7)** and shows the energies of different molecular orbitals involved in the electronic transitions of these compounds in different solvents. In the case of all the synthesized quinoxaline compounds **7a-7c, 7'a-7'c** and **8a-8c, 8'a-8'c** energy gap of the HOMO → LUMO and HOMO-1 → LUMO orbital remained

same as the solvent polarity was increased or decreased **(Tables S17-S25)**. The HOMO and LUMO as well as HOMO-1 and LUMO energy level of the compounds **7a-7'a, 7b-7'b, 7c-7'c** and **8a-8'a, 8b-8'b, 8c-8'c** in DMF it remained same, and it may be due to the very similar oxidation and reduction potential **(Figure 8)**. This is understandable because of these structural isomer having same oxidation and reduction site[38].

<< Please insert Figure 8 >>

Molecular orbital diagram of the compounds **7a-7c, 7'a-7'c** and **8a-8c, 8'a-8'c** are shown in **Tables S26-S27**. From the pictorial diagram the compounds **7a-7c, 7'a-7'c** and **8a-8c, 8'a-8'c** was found that HOMO → LUMO and HOMO-1 → LUMO orbitals are fully delocalized throughout the molecule respectively. The electron densities of the compounds **7a-7c, 7'a-7'c** and **8a-8c, 8'a-8'c** in the HOMO and HOMO-1 were slightly more located on the donor moiety 9,10-dihydrophenanthrene/ 1,2-diphenylethane/ 1-ethylindoline along with quinoxaline unit and the electron densities on the LUMOs were found localized on the acceptor end. The excitation from HOMO and HOMO-1 to LUMO mostly consists of charge transfer from the donor core to the acceptor end. **Figure 9** contains FMO of dye **7a** in the ground state, which shows that the electron densities are located on the donor 9,10-dihydrophenanthrene and quinoxaline moiety in the HOMO and these electron densities were shifted towards the acceptor moiety in the LUMO. Similar observation is seen in all the compounds **(Tables S26-S27)**.

<< Please insert Figure 9 >>

3.7. Thermal Stability

The dye molecules should form compact aggregates due to the strong intermolecular interactions so that they acquire high thermal stability[39]. In order to assess the thermal properties of the compounds,

thermal stability studies have been carried out using thermal gravimetric techniques (TGA) in the temperature range 40-600 ^{o}C under nitrogen gas at a heating rate of 10 ^{o}C min^{-1}. The TGA results indicated that the synthesized quinoxaline derivatives are stable up to 270 ^{o}C. TGA revealed the onset decomposition temperature (Td) of compounds **7a, 7b, 7c, 7'a, 7'b, 7'c, 8a, 8b, 8c, 8'a, 8'b** and **8'c** are 294 ^{o}C (99%), 275 ^{o}C (98%), 271 ^{o}C (96%), 298 ^{o}C (99%), 270 ^{o}C (98%), 273 ^{o}C (98%), 383 ^{o}C (92%), 350 ^{o}C (91%), 370 ^{o}C (82%), 385 ^{o}C (91%), 300 ^{o}C (97%) and 338 ^{o}C (97%) respectively. In general the backbones of these quinoxaline derivatives are stable up to 270 ^{o}C and above 270 ^{o}C the thermogravimetric curve of these showed a major loss in weight. The TGA results showed that quinoxaline derivatives have good thermal stability. Compounds **7a, 7b, 7'a, 7'b, 7'c, 8'b** and **8'c** showed a sharp decomposition after temperature 294 ^{o}C, 275 ^{o}C, 298 ^{o}C, 270 ^{o}C, 273 ^{o}C, 300 ^{o}C and 338 ^{o}C respectively and completely decomposed beyond 400 ^{o}C. However, the compounds **7c, 8a, 8b, 8c** and **8'a** showed sluggish decomposition nature and completely decomposed beyond 600 ^{o}C. The observations are summarized in **Figure 10.**

<< Please insert Figure 10 >>

4. Conclusion

In this paper we have reported new chemiluminescent analogues containing an inbuilt quinoxaline residue and their photophysical and chemiluminescence properties by reaction with hydrogen peroxide in the presence of potassium hexacyanoferrate (III) in an alkaline medium. The compounds **8a, 8b, 8c, 8'a, 8'b** and **8'c** can be used as promising candidate for chemiluminescent probes. Photophysical properties of the synthesized compounds **7a-7c, 7'a-7'c, 8a-8c** and **8'a-8'c** were supported by DFT and it was observed that computational results are good agreement with the theoretical observations. The synthesized compounds were confirmed by IR, ^{1}H-NMR, ^{13}C-NMR and mass spectral analysis. The

thermal stability was determined by TGA analysis and it was found that the compounds are thermally stable.

Acknowledgements

The authors are greatly thankful to TIFR, SAIF-I.I.T. Mumbai for recording the ^{1}H-NMR, ^{13}C-NMR and Mass spectra. One of the authors Mininath S. Deshmukh is grateful to CSIR for financial support.

References

[1] Todoroki K, Ohba Y, Zaitsu K. Chemiluminescence Characteristics of N-(4-Substituted Benzyl)isoluminol. Chem Pharm Bull (Tokyo) 2000;48:2011–3.

[2] Yoshida H, Ureshino K, Ishida J, Nohta H, Yamaguchi M. Chemiluminescent properties of some luminol related compounds (II). Dye Pigment 1999;41:177–82. doi:http://dx.doi.org/10.1016/S0143-7208(98)00067-9.

[3] Spurlin SR, Cooper MM. A ChemiluminesClent Precolumn Labelling Reagent for High-Performance Liquid Chromatography of Amino Acids. Anal Lett 1986;19:2277–83. doi:10.1080/00032718608064553.

[4] Steijger OM, Lingeman H, Brinkman UAT, Holthuis JJM, Smilde AK, Doornbos DA. Liquid chromatographic analysis of carboxylic acids using N-(4-aminobutyl)-N-ethylisoluminol as chemiluminescent label: determination of ibuprofen in saliva. J Chromatogr B Biomed Sci Appl 1993;615:97–110. doi:http://dx.doi.org/10.1016/0378-4347(93)80295-F.

[5] Kawasaki T, Maeda M, Tsuji A. Chemiluminescence high-performance liquid chromatography using N-(4-aminobutyl)-N-ethylisoluminol as a precolumn labelling reagent. J Chromatogr A 1985;328:121–6. doi:http://dx.doi.org/10.1016/S0021-9673(01)87383-0.

[6] Ishida J, Yamaguchi M, Nakahara T, Nakamura M. 4,5-Diaminophthalhy drazide as a highly sensitive chemiluminescence reagent for α-keto acids in liquid chromatography. Anal Chim Acta 1990;231:1–6. doi:http://dx.doi.org/10.1016/S0003-2670(00)86389-8.

[7] Ishida J, Yakabe T, Nohta H, Yamaguchi M. 6-Aminomethylphthalhydrazide as a highly sensitive chemiluminescence derivatization reagent for 5-hydroxyindoles in liquid chromatography. Anal Chim Acta 1997;346:175–81. doi:http://dx.doi.org/10.1016/S0003-2670(97)00122-0.

[8] Gundermann K-D, Drawert M. Konstitution und Chemilumineszenz, I. Sterische Resonanzhinderung bei alkylierten Amino-phthalhydraziden. Chem Ber 1962;95:2018–26. doi:10.1002/cber.19620950825.

[9] Gundermann K-D, Horstmann W, Bergmann G. Konstitution und Chemilumineszenz, II. Synthese und Chemilumineszenz-Verhalten von 7-Dialkylamino-naphthalin-dicarbonsäure-(1.2)-hydraziden. Justus Liebigs Ann Chem 1965;684:127–41. doi:10.1002/jlac.19656840115.

[10] Brock ED, Lewis DM, Yousaf TI, Harper HH. Reactive Dye Compounds. WO99/51688, 1999.

[11] Dailey S, Feast WJ, Peace RJ, Sage IC, Till S, Wood EL. Synthesis and device characterisation of side-chain polymer electron transport materials for organic semiconductor applications. J Mater Chem 2001;11:2238–43. doi:10.1039/B104674H.

[12] Kumar S. Triphenylene-based discotic liquid crystal dimers, oligomers and polymers. Liq Cryst 2005;32:1089–113. doi:10.1080/02678290500117415.

[13] Kato T, Hirai Y, Nakaso S, Moriyama M. Liquid-crystalline physical gels. Chem Soc Rev 2007;36:1857–67. doi:10.1039/B612546H.

[14] Kaafarani BR. Discotic Liquid Crystals for Opto-Electronic Applications. Chem Mater 2010;23:378–96. doi:10.1021/cm102117c.

[15] Zhou Y, He Q, Yang Y, Zhong H, He C, Sang G, et al. Binaphthyl-Containing Green- and Red-Emitting Molecules for Solution-Processable Organic Light-Emitting Diodes. Adv Funct Mater 2008;18:3299–306. doi:10.1002/adfm.200800375.

[16] Pu Y-J, Kamiya A, Nakayama K, Kido J. Arylamino-9,10-diphenylanthracenes for organic light emitting devices. Org Electron 2010;11:479–85. doi:http://dx.doi.org/10.1016/j.orgel.2009.12.001.

[17] Matsumoto N, Adachi C. Exciplex Formations at the HTL/Alq3 Interface in an Organic Light-Emitting Diode: Influence of the Electron−Hole Recombination Zone and Electric Field. J Phys Chem C 2010;114:4652–8. doi:10.1021/jp9121062.

[18] Achelle S, Baudequin C, Plé N. Luminescent materials incorporating pyrazine or quinoxaline moieties. Dye Pigment 2013;98:575–600. doi:10.1016/j.dyepig.2013.03.030.

[19] Brouwer AM. Standards for photoluminescence quantum yield measurements in solution (IUPAC Technical Report). Pure Appl Chem 2011;83:2213–28. doi:10.1351/PAC-REP-10-09-31.

[20] Treutler O, Ahlrichs R. Efficient molecular numerical integration schemes. J Chem Phys 1995;102:346.

[21] Becke A. A new mixing of Hartree-Fock and local density functional theories. J Chem Phys 1993;98:1372.

[22] Lee, Chengteh and Yang, Weitao and Parr RG. Development of the Colle-Salvetti correlation-energy formula into a functional of the electron density. Phys Rev B 1988;37:785–9. doi:10.1103/PhysRevB.37.785.

[23] Kim CH, Park J, Seo J, Park SY, Joo T. Excited State Intramolecular Proton Transfer and Charge Transfer Dynamics of a 2-(2′-Hydroxyphenyl)benzoxazole Derivative in Solution. J Phys Chem A 2010;114:5618–29. doi:10.1021/jp909438p.

[24] Santra M, Moon H, Park M-H, Lee T-W, Kim YK, Ahn KH. Dramatic Substituent Effects on the Photoluminescence of Boron Complexes of 2-(Benzothiazol-2-yl)phenols. Chem – A Eur J 2012;18:9886–93. doi:10.1002/chem.201200726.

[25] Casida ME, Jamorski C, Casida KC, Salahub DR. Molecular excitation energies to high-lying bound states from time-dependent density-functional response theory: Characterization and correction of the time-dependent local density approximation ionization threshold. J Chem Phys 1998;108:4439.

[26] Li H, Niu L, Xu X, Zhang S, Gao F. A Comprehensive Therotical Investigation of Intramolecular Proton Transfer in the Excited States for Some Newly-designed Diphenylethylene Derivatives Bearing 2-(2-Hydroxy-Phenyl)-Benzotriazole Part. J Fluoresc 2011;21:1721–8. doi:10.1007/s10895-011-0867-6.

[27] Bauernschmitt R, Ahlrichs R. Treatment of electronic excitations within the adiabatic approximation of time dependent density functional theory. Chem Phys Lett 1996;256:454–64. doi:http://dx.doi.org/10.1016/0009-2614(96)00440-X.

[28] Furche F, Rappoport D. Density functional theory for excited states: Equilibrium structure and electronic spectra. In Computational Photochemistry. In: Olivucci M, editor. Comput. Photochem., Amsterdam: Elsevier; 2005, p. 93.

[29] Wiberg KB. Ab Initio Molecular Orbital Theory by W. J. Hehre, L. Radom, P. v. R. Schleyer, and J. A. Pople, John Wiley, New York, 548pp. Price: 79.95 (1986). J Comput Chem 1986;7:379. doi:10.1002/jcc.540070314.

[30] Lakowicz JR. Principles of Fluorescence Spectroscopy, 2nd ed. New York: Kluwer Academic; 1999.

[31] Valeur B. Molecular Fluorescence: Principles and Applications. Weinheim: Wiley-VCH Verlag GmbH; 2001.

[32] Cossi M, Barone V, Cammi R, Tomasi J. Ab initio study of solvated molecules: a new implementation of the polarizable continuum model. Chem Phys Lett 1996;255:327–35. doi:http://dx.doi.org/10.1016/0009-2614(96)00349-1.

[33] Frisch MJ, Trucks GW, Schlegel HB, Scuseria GE, Robb MA, Cheeseman JR, et al. Gaussian 09 C.01 2009.

[34] Williams RL, Shalaby SW. Heterocyclic studies: New heterocyclic ring systems from isomeric dimethyl diaminophthalates. J Heterocycl Chem 1973;10:891–8. doi:10.1002/jhet.5570100602.

[35] Tyagi P, Venkateswararao A, Thomas KRJ. Solution Processable Indoloquinoxaline Derivatives Containing Bulky Polyaromatic Hydrocarbons: Synthesis, Optical Spectra, and Electroluminescence. J Org Chem 2011;76:4571–81. doi:10.1021/jo2004764.

[36] Yoshida H, Nakao R, Nohta H, Yamaguchi M. Chemiluminescent properties of some luminol-related compounds — Part 3. Dye Pigment 2000;47:239–45. doi:http://dx.doi.org/10.1016/S0143-7208(00)00080-2.

[37] Dennington R, Keith T MJ. Gaussview version 5.0 2009.

[38] Chen C-T, Chiang C-L, Lin Y-C, Chan L-H, Huang, Tsai Z-W, et al. Ortho-Substituent Effect on Fluorescence and Electroluminescence of Arylamino-Substituted Coumarin and Stilbene. Org Lett 2003;5:1261–4. doi:10.1021/ol034268h.

[39] Chunlong Z, Nianchun M, Liyun L. An investigation of the thermal stability of some yellow and red azo pigments. Dye Pigment 1993;23:13–23. doi:http://dx.doi.org/10.1016/0143-7208(93)80020-2.